Journal of Photochemistry and Photobiology A: Chemistry 210 (2010) 77–81

Contents lists available at ScienceDirect

Journal of Photochemistry and Photobiology A: Chemistry

journal homepage: www.elsevier.com/locate/jphotochem

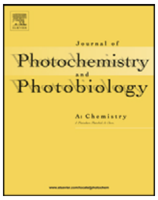

Time-dependent density functional theory study of the excited-state dihydrogen bond O–H···H–Si

Ningning Wei[a], Peng Li[b,*], Ce Hao[a,*], Rui Wang[a], Zhilong Xiu[a], Jingwen Chen[a], Peng Song[b,*]

[a] School of Environmental and Biological Science and Technology, State Key Laboratory of Fine Chemicals, Dalian University of Technology, Dalian 116024, China
[b] State Key Laboratory of Molecular Reaction Dynamics, Dalian Institute of Chemical Physics, Chinese Academy of Sciences, 457 Zhongshan Road, Dalian 116023, China

ARTICLE INFO

Article history:
Received 2 June 2009
Received in revised form
17 November 2009
Accepted 2 December 2009
Available online 11 December 2009

Keywords:
Dihydrogen bond
Infrared spectra
Electronically excited state
Time-dependent density functional theory

ABSTRACT

Intermolecular dihydrogen bonding in the electronically excited states of a phenol–diethylmethylsilane (DEMS) complex was studied theoretically using the time-dependent density functional theory (TDDFT) method. Analysis of the frontier molecular orbitals revealed a locally excited S_1 state for the dihydrogen-bonded phenol–DEMS complex in which only the phenol moiety is electronically excited. The calculated infrared spectrum of the phenol–DEMS complex is quite different from that of previously studied S_1 state of a dihydrogen-bonded phenol–borane-trimethylamine complex. The O–H and Si–H stretching vibrational modes appear as intense, sharp peaks for the S_1 state which are slightly red-shifted compared with those predicted for the ground state. Upon electronic excitation to the S_1 state, the O–H and Si–H bonds involved in the dihydrogen bond O–H···H–Si lengthen slightly, while the C–O bond shortens. The calculated H···H distance is significantly shorter in the S_1 state than in the ground state. Thus, the intermolecular dihydrogen bond of the phenol–DEMS complex is stronger in the electronically excited state than in the ground state.

1. Introduction

Over the last decades, the hydrogen bond has gained wide attention because of its importance in physical, chemical and biological processes [1–51]. The conventional hydrogen bond is an analogous interaction X–H···A formed by a strongly polar group $X^{\delta-}$–$H^{\delta+}$ on one side, and atom $A^{\delta-}$ with a lone pair of electrons on the other side [1–22]. As the study of hydrogen bonds has progressed, some unconventional hydrogen bonds have been proposed using diverse experimental techniques and theoretical calculations. Another type of hydrogen bond, formed between two oppositely charged hydrogen atoms, is called the dihydrogen bond [23–51]. It can be represented as $X–H^{\delta-}\cdots{}^{\delta+}H–Y$, where X and Y are electropositive and electronegative atoms respectively [23–29]. The electrostatic attraction between oppositely polarized hydrogen atoms promotes the formation of the dihydrogen bond and maintains its stability [25–35]. With comparative strength and directionality to conventional hydrogen bonding, dihydrogen bonding can influence the structure, reactivity and selectivity of compounds in gas and condensed phases. Thus, it has potential application in catalysis, crystal engineering and materials chemistry [23–49].

Dihydrogen bonding is now a well-established interaction and found in various complexes. Mikami and co-workers have reported the formation of several dihydrogen-bonded complexes between borane amines and molecules containing acidic hydrogen atoms in the gas phase [36–45]. Recently, Zhao and Han [49] reported the theoretical study on the structure and dynamics of a novel dihydrogen bond in the electronically excited state of a phenol–borane-trimethylamine (BTMA) complex for the first time. In their landmark work, their calculated results reveal that the dihydrogen-bonded phenol–BTMA complex possesses a locally excited (LE) S_1 state that is centered on the phenol moiety. In addition, there is no O–H or B–H stretching vibrational mode in the calculated infrared (IR) spectrum of the S_1 state of the dihydrogen-bonded phenol–BTMA complex. This was attributed to the strengthening of the dihydrogen bond O–H···H–B in the electronically excited state.

Ishikawa et al. [47] reported the first experimental observation of a dihydrogen bond involving a Si–H group in a phenol–diethylmethylsilane (DEMS) complex. This complex should be a good precursor for H_2 elimination reactions. IR-UV double-resonance spectroscopy was performed to identify the dihydrogen bond containing the Si–H group. When DEMS was added to gaseous phenol, many small bands appeared in the vicinity of the origin band attributed to the phenol monomer in the fluorescence excitation spectrum. Three isomers of the complex were identified by IR-UV population labeling spectroscopy and laser-induced fluorescence spectroscopy. The electronic ori-

---

* Corresponding authors. Tel.: +86 411 83699167; fax: +86 411 84675584.
E-mail addresses: pengl@dicp.ac.cn (P. Li), haoce@dlut.edu.cn (C. Hao).

1010-6030/$ – see front matter © 2009 Elsevier B.V. All rights reserved.
doi:10.1016/j.jphotochem.2009.12.001

gin band of the phenol–DEMS complex shifts by −78 to +4 cm^{-1} compared with that of the phenol monomer. The IR absorption spectra of the phenol–DEMS isomers show that the O–H stretching vibration frequencies shift to lower frequency by 21–29 cm^{-1}. The magnitudes of these shifts are much smaller than those calculated for the phenol–borane-dimethylamine (−174 cm^{-1}) [38] and phenol–BTMA (−143 cm^{-1}) complexes [39]. To obtain structural information about the dihydrogen-bonded phenol–DEMS complex, Ishikawa et al. performed quantum-chemical calculations together with experimental measurements. The calculation showed there were five stable isomers in the ground state. For three isomers, the distance between the two hydrogen atoms involved in the dihydrogen bonds ($R_{H\cdots H}$) is 2.23 Å, and the O–H vibrational frequency (ν_{OH}) is 3641 cm^{-1}. The $R_{H\cdots H}$ and ν_{OH} of the other two isomers are 2.27 Å and 3640 cm^{-1}, and 2.27 Å and 3641 cm^{-1}, respectively. Further spectroscopic investigations and theoretical calculations are still required for various dihydrogen-bonded complexes to fully understand the properties of the dihydrogen bond, such as geometric conformation and its potential utility. Tremendous effort has been spent investigating the ground state properties of dihydrogen bonds in dihydrogen-bonded complexes. In contrast, research focused on the structure and dynamics of dihydrogen bonds in electronically excited states is scarce. In this study, theoretical calculations have been performed to investigate the properties of the dihydrogen bond in an electronically excited state of a dihydrogen-bonded phenol–DEMS complex. The five isomers proposed by Ishikawa et al. for this complex have similar geometries. The geometry of isomer 1 reported by Ishikawa et al. was used in the present work as it possesses the lowest relative energy and has a $R_{H\cdots H}$ of 2.23 Å. Time-dependent density functional theory (TDDFT) was used for excited-state geometry optimization and electronic transition calculations for the dihydrogen-bonded phenol–DEMS complex and the isolated monomers. TDDFT has been proven a valid tool for calculating the IR spectra of the electronically excited state of compounds [9–22]. Here, TDDFT is used to predict the excited-state IR spectra of both the O–H and Si–H stretching vibrational regions of the dihydrogen-bonded phenol–DEMS complex.

2. Computational methods

Density functional theory (DFT) and time-dependent density functional theory (TDDFT) were employed for our ground state and excited state computations, respectively [49–52]. The resolution-of-the-identity (RI) approximation was adopted in the purpose of improving efficiency without sacrificing accuracy of the results [53–55]. All geometry optimizations were carried out using BP-86 functional with triple zeta valence plus polarization (TZVP) basis set as well as corresponding auxiliary basis sets for resolution-of-the-identity (RI) approximation [56]. Harmonic vibrational frequency analysis was performed at the same theoretical level [54–57]. All the computations were performed using the TURBOMOLE program suite.

3. Results and discussion

The optimized geometry of the dihydrogen-bonded phenol–DEMS complex in the ground state is shown in Fig. 1. In the ground state, the dihydrogen bond O–$H_1\cdots H_2$–Si is formed between phenol and DEMS. Table 1 lists the calculated bond lengths, angles and dihedral angle of isolated phenol and DEMS and the dihydrogen-bonded phenol–DEMS complex in the ground state. The calculated distance between the two hydrogen atoms $H_1\cdots H_2$ is 1.841 Å, which is slightly longer than that of the dihydrogen-bonded phenol–BTMA complex (1.737 Å) [49]. The bond angles O–$H_1\cdots H_2$ and $H_1\cdots H_2$–Si for the optimized conformation of the phenol–DEMS complex are 170.8° and 138.3°, respectively. The dihedral angle O–$H_1\cdots H_2$–Si is 46.65°. Furthermore, the calculated bond length for the O–H_1 group is 0.976 Å in the dihydrogen-bonded phenol–DEMS complex, which is slightly longer than that of the O–H_1 group in isolated phenol (0.973 Å). At the same time, the bond length for C_1–O in the phenol–DEMS complex (1.360 Å) is slightly shorter than that in free phenol (1.376 Å). In the DEMS moiety, the Si–H_2 bond lengthens and the Si–$C_{7,8,10}$ bonds shorten upon formation of the intermolecular dihydrogen bond. These results are similar to those observed for the dihydrogen-bonded phenol–BTMA complex.

The electronic transition energies and corresponding oscillator strengths for the low-lying electronically excited states of the dihydrogen-bonded phenol–DEMS complex and the isolated monomers were calculated using TDDFT. The results are listed in Table 2. All of the electronic transition energies of the dihydrogen-bonded complex are just a little higher than those of isolated phenol, but significantly lower than those of free DEMS. The phenol–DEMS complex exhibits phenol-based elec-

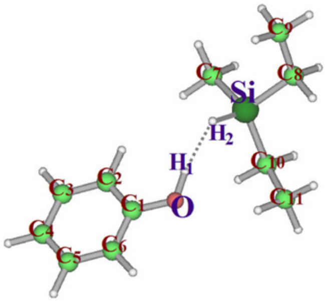

Fig. 1. Optimized geometry of the dihydrogen-bonded phenol–DEMS complex in the ground state. The dotted line denotes the intermolecular dihydrogen bond.

Table 1
Calculated bond lengths (Å), angles (°) and dihedral angle (°) of the isolated monomers and the dihydrogen-bonded phenol–DEMS complex in the ground state.

	Phenol[a]	DEMS	Phenol–DEMS
C_1–O	1.376	–	1.360
O–H_1	0.973	–	0.976
$H_1\cdots H_2$	–	–	1.841
H_2–Si	–	1.506	1.514
O–$H_1\cdots H_2$	–	–	170.8
$H_1\cdots H_2$–Si	–	–	138.3
O–$H_1\cdots H_2$–Si	–	–	46.65
Si–C_7	–	1.896	1.893
Si–C_8	–	1.904	1.900
Si–C_{10}	–	1.903	1.899

[a] Data taken from Ref. [49].

Table 2
Calculated electronic transition energies (eV) and corresponding oscillator strengths (in parentheses) for the low-lying electronically excited states of the dihydrogen-bonded phenol–DEMS complex and the isolated monomers. The contributions of the orbital transitions for the S_1 state are also listed.

	Phenol–DEMS	Phenol[a]	DEMS
S_1	5.114(0.033) H → L 80.2% H-1 → L+1 19.3%	4.789(0.031) H → L 82.5% H-1 → L+1 16.7%	8.010(0.008) H → L 91.3%
S_2	5.967(0.058)	5.684(0.049)	8.134
S_3	6.208(0.000)	5.782(0.000)	8.336
S_4	6.509(0.003)	6.467(0.001)	8.486
S_5	6.812(0.208)	6.508(0.215)	8.514
S_6	6.944(0.519)	6.575(0.002)	8.746

H: highest occupied molecular orbital (HOMO), L: lowest unoccupied molecular orbital (LUMO).

[a] Data taken from Ref. [49].

tronic transitions that are blue-shifted compared with that of free phenol, i.e., the electronic transitions of phenol increase in energy upon formation of the intermolecular dihydrogen bond. The electronic transition energy for the S_1 state of the dihydrogen-bonded phenol–DEMS complex (5.114 eV) is close to that of the phenol monomer (4.789 eV), which is much lower than the transition energy for S_1 state of isolated DEMS (8.010 eV). This infers that the electronically excited state of the dihydrogen-bonded phenol–DEMS complex is localized on the phenol molecule, while the DEMS molecule remains in the ground state. The orbital transition contributions for the S_1 state of the phenol–DEMS complex are also presented in Table 2. Two main orbital transitions contribute to the S_1 state: one is from the highest occupied molecular orbital (HOMO) to the lowest unoccupied molecular orbital (LUMO) (80.2%), the other is from the HOMO-1 to the LUMO+1 (19.3%). Thus, it can be concluded that four main orbitals are involved in the S_1 state of the dihydrogen-bonded phenol–DEMS complex. This finding varies from the S_1 state of the dihydrogen-bonded phenol–BTMA complex which involves three molecular orbitals: the HOMO, LUMO and LUMO+1.

Molecular orbital (MO) analysis can directly provide insight into the nature of the excited states [58–64]. The frontier MOs of the dihydrogen-bonded phenol–DEMS complex are depicted in Fig. 2. Here, only the HOMO-1, HOMO, LUMO and LUMO+1 orbitals are shown because the S_1 state of the complex is associated with these four orbitals. The electron densities of all four orbitals are localized on the phenol moiety. Hence, the S_1 state of the dihydrogen-bonded phenol–DEMS complex is a LE state. This result is consistent with our earlier speculation that only the phenol moiety is excited in the S_1 state of the dihydrogen-bonded phenol–DEMS complex. From Fig. 2, one can visualize electronic excitation between the π–π^* orbitals of the benzene ring and the lone electron pair on the hydroxyl group. Thus, both the dihydrogen bond $O–H_1\cdots H_2–Si$ and the phenol moiety in the dihydrogen-bonded phenol–DEMS complex should be strongly influenced by charge redistribution in the S_1 state, which is similar to that of the dihydrogen-bonded phenol–BTMA complex.

The excited-state geometry optimizations for the dihydrogen-bonded phenol–DEMS complex and the isolated monomers were performed using TDDFT. Based on the optimized structures, the IR spectra for both the ground state and the S_1 state were calculated. Changes in the intermolecular dihydrogen bonding $O–H_1\cdots H_2–Si$ between the different states can be monitored by shifts in the O–H and Si–H stretching vibrational modes in the IR spectra. The calculated IR spectra for the dihydrogen-bonded phenol–DEMS complex and isolated monomers in different electronic states are shown in Fig. 3. All of the O–H and Si–H stretching vibration frequencies are labeled in Fig. 3. The O–H stretching vibration frequency of isolated phenol in the ground state (3692 cm^{-1}) was calculated by Zhao and Han [49]. The calculated stretching vibration frequency for the O–H bond in the dihydrogen-bonded phenol–DEMS complex shifts to 3596 cm^{-1} because of the formation of the dihydrogen bond $O–H_1\cdots H_2–Si$. The magnitude of the shift (96 cm^{-1}) is much smaller than that calculated for the dihydrogen-bonded phenol–BTMA complex (202 cm^{-1}) [49]. This indicates that the dihydrogen bond O–H···H–Si is not as strong as the dihydrogen bond O–H···H–B in the ground state. The stretching vibration frequency at 2140 cm^{-1} can be assigned to the Si–H vibrational mode of the complex, which is shifted to a lower frequency by 45 cm^{-1} relative to free DEMS. Furthermore, in the S_1 state, the O–H stretching vibrational mode of the dihydrogen-bonded phenol–DEMS complex shows a red shift of 145 cm^{-1} compared with the ground state, indicating that the $O–H_1$ bond lengthens upon electronic excitation. The Si–H group of the dihydrogen-bonded phenol–DEMS complex exhibits a relatively small red shift from the ground state (2140 cm^{-1}) to the S_1 state (2117 cm^{-1}). Therefore, the length of the $Si–H_2$ bond may not increase as much as the $O–H_1$ bond upon electronic excitation. The changes in the $O–H_1$ and $Si–H_2$ bonds suggest that the dihydrogen bond $O–H_1\cdots H_2–Si$ should be stronger in the S_1 state than the ground state. The IR signals of the O–H and Si–H groups involved in dihydrogen bonding are intense and sharp in the S_1 state. This is quite different behavior from that of the S_1 state of the dihydrogen-bonded phenol–BTMA complex. The stretching vibrational bands of the O–H and B–H bonds of the dihydrogen-bonded phenol–BTMA complex both disappeared in the S_1 state, followed by a strong vibrational absorption appearing in the region of a C═O stretching vibration [49]. The differences between the excited state behavior of the two complexes suggest that the $O–H_1$ and $Si–H_2$ bonds of the dihydrogen-bonded phenol–DEMS complex may be lengthened less than the O–H and B–H bonds of the dihydrogen-bonded phenol–BTMA complex upon electronic excitation.

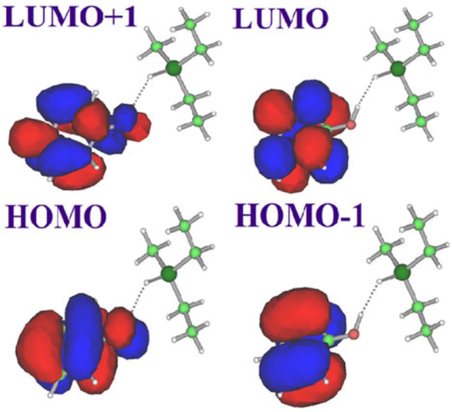

Fig. 2. Frontier MOs of the dihydrogen-bonded phenol–DEMS complex.

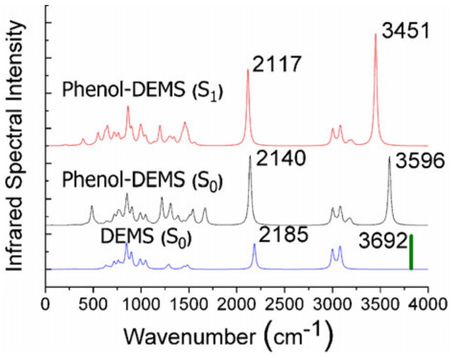

Fig. 3. Calculated IR spectra of the dihydrogen-bonded phenol–DEMS complex and DEMS in different electronic states. The thick green line denotes the stretching vibrational frequency of the hydroxyl group in isolated phenol [49]. (For interpretation of the references to color in this figure legend, the reader is referred to the web version of the article.)

Table 3 lists all the bond lengths, angles and the dihedral angles of the dihydrogen bond for different electronic states of the phenol–DEMS complex. The $C_1–O$ bond shortens by 0.016 Å in the ground-state phenol–DEMS complex due to formation of the intermolecular dihydrogen bond. Upon electronic excitation to the S_1 state in the dihydrogen-bonded phenol-DEMS complex, the $C_1–O$ and $O–H_1$ bonds change by −0.014 and +0.009 Å, respectively. These changes are much smaller than those found for the dihydrogen-bonded phenol–BTMA complex. These findings are consistent with the IR spectra of the dihydrogen-bonded phenol–DEMS complex, because the S_1 state exhibits an O–H stretching band that does not show C═O bond character. For the DEMS moiety of the complex in ground state, the $Si–H_2$ bond lengthens slightly by 0.008 Å after formation of the intermolec-

Table 3
Calculated bond lengths (Å), angles (°) and dihedral angles (°) of the dihydrogen-bonded phenol–DEMS complex in the ground state (GS) and the electronically excited state (ES).

	Phenol–DEMS	
	GS	ES
C_1–O	1.360	1.346
O–H_1	0.976	0.985
$H_1\cdots H_2$	1.841	1.712
H_2–Si	1.514	1.518
O–$H_1\cdots H_2$	170.8	171.5
$H_1\cdots H_2$–Si	138.3	132.0
O–$H_1\cdots H_2$–Si	46.65	76.32
Si–C_7	1.893	1.891
Si–C_8	1.900	1.900
Si–C_{10}	1.899	1.898
C_1–C_2	1.404	1.434
C_2–C_3	1.399	1.430
C_3–C_4	1.398	1.422
C_4–C_5	1.401	1.420
C_5–C_6	1.396	1.431
C_6–C_1	1.404	1.421
C_8–C_9	1.538	1.538
C_{10}–C_{11}	1.539	1.539

ular dihydrogen bond. Upon electronic excitation to the S_1 state of the dihydrogen-bonded phenol–DEMS complex, the Si–H_2 bond lengthens by only 0.004 Å and the Si–$C_{7,8,10}$ bonds hardly change. Thus the Si–H stretching vibrational absorption in the S_1 state is still observed in Fig. 3, but a stretching vibrational mode in the region of a carbonyl group is not. The distance $H_1\cdots H_2$ in the dihydrogen-bonded phenol–DEMS complex shortens significantly by 0.129 Å in the S_1 state compared with the ground state. This finding is consistent with the results of the calculated IR spectra which implied that the dihydrogen bond strengthens upon excitation to the S_1 state. The O–$H_1\cdots H_2$ and $H_1\cdots H_2$–Si bond angles increase and decrease by only +0.7° and −6.3°, respectively, between the ground and the S_1 state. However, the dihedral angle O–$H_1\cdots H_2$–Si increases significantly upon excitation from the ground state (46.65°) to the S_1 state (76.32°). The dihedral angle of the S_1 state results in the phenol and DEMS molecules becoming almost perpendicular to each other. The variations of the bond angles and dihedral angles between the S_0 state and the S_1 state are attributed to conformational changes in the complex upon electronic excitation. However, the conformation of the dihydrogen-bonded phenol–DEMS complex does not change as much as that of the dihydrogen-bonded phenol–BTMA complex upon excitation from the S_0 state to the S_1 state. Thus, it is postulated that the dihydrogen bond O–H···H–B is stronger than O–H···H–Si in the S_1 state of the respective complexes. Furthermore, all the C–C bonds of the phenol benzene ring lengthen upon electronic excitation, while the Si–$C_{7,8,10}$ and C–C bonds of the DEMS moiety are almost unchanged. The conformational changes of the benzene ring can be attributed to the LE state on the phenol moiety.

4. Conclusion

In this study, the electronic excited state properties of a dihydrogen-bonded phenol–DEMS complex were investigated by TDDFT. An intermolecular dihydrogen bond O–H···H–Si existed between the phenol and DEMS molecules in the optimized geometry of the phenol–DEMS complex. According to the calculated electronic transition energies, the electronic transitions of the dihydrogen-bonded phenol–DEMS complex are blue-shifted compared with that of isolated phenol as a result of the formation of the intermolecular dihydrogen bond. Analysis of the frontier MOs revealed that the S_1 state of the dihydrogen-bonded phenol–DEMS complex is a LE state centered on the phenol moiety. The dihydrogen-bonded phenol–BTMA complex also exhibits a LE S_1 state. The IR spectra of the S_0 and S_1 states of the dihydrogen-bonded phenol–DEMS complex were also calculated. Vibrational absorption bands associated with the O–H and Si–H bonds of the dihydrogen-bonded phenol–DEMS complex were slightly red shifted upon excitation to the S_1 state. Moreover, the O–H_1 and Si–H_2 bonds were both longer in the S_1 state relative to those in the ground state. However, the C_1–O bond shortens slightly and the Si–$C_{7,8,10}$ bonds remain almost unchanged upon electronic excitation. Thus, the excited state IR spectra of the dihydrogen-bonded phenol–DEMS complex exhibit strong, sharp peaks for the O–H and Si–H stretching vibrational modes, and do not show C=O character. The C–C bonds of the benzene ring increase in length because of the LE state centered on the phenol moiety. The $H_1\cdots H_2$ distance of the dihydrogen bond is much shorter in the S_1 state than in the ground state. It can be concluded that the intermolecular dihydrogen bond O–H···H–Si of the dihydrogen-bonded phenol–DEMS complex is stronger in the S_1 excited state. In addition, the dihydrogen bond is stronger in a phenol–borane-amine complex than in the corresponding phenol–silane complex both in the ground and electronically excited state. Understanding the excited state properties of the dihydrogen bond continues as an area of intense experimental and theoretical research.

Acknowledgement

This work was supported by the National Natural Science Foundation of China (Grant Nos. 20773018) and the Key Laboratory of Industrial Ecology and Environmental Engineering, China Ministry of Education.

References

[1] G.A. Jeffrey, An Introduction to Hydrogen Bonding, Oxford University press, Oxford, 1997.

[2] Y. Liu, J. Ding, R. Liu, D. Shi, J. Sun, Revisiting the electronic excited-state hydrogen bonding dynamics of coumarin chromophore in alcohols: undoubtedly strengthened not cleaved, J. Photochem. Photobiol. A: Chem. 201 (2009) 203–207.

[3] C. Desfrançois, S. Carles, J.P. Schermann, Weakly bound clusters of biological interest, Chem. Rev. 100 (2000) 3943–3962.

[4] K.-L. Han, G.-Z. He, Photochemistry of aryl halides: photodissociation dynamics, J. Photochem. Photobiol. C: Photochem. Rev. 8 (2007) 55–66.

[5] T. Steiner, The hydrogen bond in the solid state, Angew. Chem. Int. Ed. 41 (2002) 48–76.

[6] G.-J. Zhao, Y.-H. Liu, K.-L. Han, Y. Dou, Dynamic simulation study on ultrafast excited-state torsional dynamics of 9, 9′-bianthryl (BA) in gas phase: real-time observation of novel oscillation behavior with the torsional coordinate, Chem. Phys. Lett. 453 (2008) 29–34.

[7] A.L. Sobolewski, W. Domcke, Intramolecular hydrogen bonding in the $S_1(\pi\pi^*)$ excited state of anthranilic acid and salicylic acid: TDDFT calculation of excited-state geometries and infrared spectra, J. Phys. Chem. A 108 (2004) 10917–10922.

[8] Y.S. Djikaeva, E. Ruckenstein, A probabilistic approach to the effect of hydrogen bonding on the hydrophobic attraction, J. Chem. Phys. 130 (2009) 124713.

[9] G.-J. Zhao, K.-L. Han, Y.-B. Lei, Y. Dou, Ultrafast excited-state dynamics of tetraphenylethylene (TPE) studied by semiclassical simulation, J. Chem. Phys. 127 (2007) 094307.

[10] S. Perun, A.L. Sobolewski, W. Domcke, Role of electron-driven proton-transfer processes in the excited-state deactivation of the adenine−thymine base pair, J. Phys. Chem. A 110 (2006) 9031–9038.

[11] G.-J. Zhao, K.-L. Han, Early time hydrogen-bonding dynamics of photoexcited coumarin 102 in hydrogen-donating solvents: theoretical study, J. Phys. Chem. A 111 (2007) 2469–2474.

[12] G.-J. Zhao, K.-L. Han, Ultrafast hydrogen bond strengthening of the photoexcited fluorenone in alcohols for facilitating the fluorescence quenching, J. Phys. Chem. A 111 (2007) 9218–9223.

[13] G.-J. Zhao, J.-Y. Liu, L.-C. Zhou, K.-L. Han, Site-selective photoinduced electron transfer from alcoholic solvents to the chromophore facilitated by hydrogen bonding: a new fluorescence quenching mechanism, J. Phys. Chem. B 111 (2007) 88940–88945.

[14] G.-J. Zhao, K.-L. Han, Site-specific solvation of the photoexcited protochlorophyllide a in methanol: formation of the hydrogen-bonded intermediate state induced by hydrogen bond strengthening, Biophys. J. 94 (2008) 38–46.

[15] G.-J. Zhao, K.-L. Han, Time-dependent density functional theory (tddft) study on the hydrogen-bonded intramolecular charge-transfer excited state of 4-

dimethylamino-benzonitrile (DMABN) in methanol, J. Comput. Chem. 29 (2008) 2010–2017.

[16] G.-J. Zhao, K.-L. Han, Effects of hydrogen bonding on tuning photochemistry: concerted hydrogen bond strengthening and weakening, Chemphyschem 9 (2008) 1842–1846.

[17] G.-J. Zhao, R.-K. Chen, M.-T. Sun, G.-Y. Li, J.-Y. Liu, Y.-L. Gao, K.-L. Han, X.-C. Yang, L.-C. Sun, Photoinduced intramolecular charge transfer in thiophene-π-conjugated donor-acceptor systems: combined experimental and TDDFT studies, Chem. Eur. J. 14 (2008) 6935–6947.

[18] K. Tsumura, K. Furuya, A. Sakamoto, M. Tasumi, Vibrational analysis of trans-stilbene in the excited singlet state by time-dependent density functional theory: calculations of the Raman, infrared, and fluorescence excitation spectra, J. Raman Spectrosc. 39 (2008) 1584–1591.

[19] G.-J. Zhao, K.-L. Han, Excited-state electronic structures and photochemistry of heterocyclic annulated perylenes (HAPs) materials tuned by heteroatoms: S, Se, N, O, C, Si, and B, J. Phys. Chem. A 113 (2009) 4788–4794.

[20] S. Chai, G.-J. Zhao, P. Song, S.-Q. Yang, J.-Y. Liu, K.-L. Han, Excited-state double proton transfer (ESDPT) in 2-aminopyridine/acid systems: role of the intermolecular hydrogen bonding in excited states, Phys. Chem. Chem. Phys. 11 (2009) 4385–4390.

[21] G.-J. Zhao, K.-L. Han, Role of intramolecular and intermolecular hydrogen bonding in both singlet and triplet excited states of aminofluorenones on internal conversion, intersystem crossing, and twisted intramolecular charge transfer, J. Phys. Chem. A (2009), doi:10.1021/jp903200x.

[22] G.-J. Zhao, K.-L. Han, Chapter 5: hydrogen bonding effects on the photochemistry of chromophores in solution, in: A. Sánchez, S.J. Gutierrez (Eds.), Photochemistry Research Progress, Nova Science Publishers, Inc., New York, 2008, pp. 161–190, ISBN: 978-1-60456-568-3.

[23] R.H. Crabtree, O. Eisenstein, G. Sini, E. Peris, New types of hydrogen bonds, J. Org. Chem. 567 (1998) 7–11.

[24] E. Fujimaki, A. Fujii, T. Ebata, N. Mikami, Autoionization-detected infrared spectroscopy of intramolecular hydrogen bonds in aromatic cations. II. Unconventional intramolecular hydrogen bonds, J. Chem. Phys. 112 (2000) 137–148.

[25] L.M. Epstein, E.S. Shubina, New types of hydrogen bonding in organometallic chemistry, Coord. Chem. Rev. 231 (2002) 165–181.

[26] R. Custelcean, J.E. Jackson, Dihydrogen bonding: structures, energetics, and dynamics, Chem. Rev. 101 (2001) 1963–1980.

[27] T.-S. Chu, Y. Zhang, K.-L. Han, The time-dependent quantum wave packet approach to the electronically nonadiabatic processes in chemical reactions, Int. Rev. Phys. Chem. 25 (2006) 201–235.

[28] G.-J. Zhao, K.-L. Han, P.J. Stang, Theoretical insights into hydrogen bonding and its influence on the structural and spectral properties of aquo palladium(II) complexes: cis-$[(\mathrm{dppp})\mathrm{Pd}(\mathrm{H_2O})_2]^{2+}$, cis-$[(\mathrm{dppp})\mathrm{Pd}(\mathrm{H_2O})(\mathrm{OSO_2CF_3})]+(\mathrm{OSO_2CF_3})^-$, and cis-$[(\mathrm{dppp})\mathrm{Pd}(\mathrm{H_2O})_2]^{2+}(\mathrm{OSO_2CF_3})^-{}_2$, J. Chem. Theory Comput. 5 (2009) 1955–1958.

[29] C.F. Matta, J. Hernández-Trujillo, T.-H. Tang, R.F.W. Bader, Hydrogen-hydrogen bonding: a stabilizing interaction in molecules and crystals, Chem. Eur. J. 9 (2003) 1940–1951.

[30] S. Marincean, J.E. Jackson, Quest for IR-pumped reactions in dihydrogen-bonded complexes, J. Phys. Chem. A 108 (2004) 5521–5526.

[31] N.V. Belkova, E.S. Shubina, L.M. Epstein, Diverse world of unconventional hydrogen bonds, Acc. Chem. Res. 38 (2005) 624–631.

[32] J. Fanfrlífk, M. Lepšik, D. Horinek, Z. Havlas, P. Hobza, Interaction of carboranes with biomolecules: formation of dihydrogen bonds, Chemphyschem 7 (2006) 1100–1105.

[33] W.T. Klooster, T.F. Koetzle, P.E.M. Siegbahn, T.B. Richardson, R.H. Crabtree, Study of the N–H···H–B dihydrogen bond including the crystal structure of $\mathrm{BH_3NH_3}$ by neutron diffraction, J. Am. Chem. Soc. 121 (1999) 6337–6343.

[34] K.-L. Han, G.-Z. He, N.-Q. Lou, Effect of location of energy barrier on the product alignment of reaction $A+BC$, J. Chem. Phys. 105 (1996) 8699–8704.

[35] T. Kar, S. Scheiner, Comparison between hydrogen and dihydrogen bonds among $\mathrm{H_3BNH_3}$, $\mathrm{H_2BNH_2}$, and $\mathrm{NH_3}$, J. Chem. Phys. 119 (2003) 1473–1482.

[36] T. Ebata, N. Mizuochi, T. Watanabe, N. Mikami, OH stretching vibrations of phenol–$(\mathrm{H_2O})_1$ and phenol–$(\mathrm{H_2O})_3$ in the S_1 state, J. Phys. Chem. 100 (1996) 546–550.

[37] A. Iwasaki, A. Fujii, T. Watanabe, T. Ebata, N. Mikami, Infrared spectroscopy of hydrogen-bonded phenol–amine clusters in supersonic jets, J. Phys. Chem. 100 (1996) 16053–16057.

[38] G. Naresh Patwari, T. Ebata, N. Mikami, Evidence of a dihydrogen bond in gas phase: phenol–borane-dimethylamine complex, J. Chem. Phys. 113 (2000) 9885–9888.

[39] G. Naresh Patwari, T. Ebata, N. Mikami, Gas phase dihydrogen bonded phenol–borane-trimethylamine complex, J. Chem. Phys. 114 (2001) 8877–8879.

[40] G. Naresh Patwari, T. Ebata, N. Mikami, Dihydrogen bonded phenol–borane-dimethylamine complex: an experimental and theoretical study, J. Chem. Phys. 116 (2002) 6056–6063.

[41] G. Naresh Patwari, T. Ebata, N. Mikami, Dehydrogenation reaction from a dihydrogen bonded precursor complex in the gas phase, J. Phys. Chem. A 105 (2001) 10753–10758.

[42] G. Naresh Patwari, T. Ebata, N. Mikami, Gas phase dihydrogen bonding: clusters of borane-amines with phenol and aniline, Chem. Phys. 283 (2002) 193–207.

[43] G. Naresh Patwari, Proton affinities of borane-amines: consequences on dihydrogen bonding, J. Phys. Chem. A 109 (2005) 2035–2038.

[44] G. Naresh Patwari, A. Fujii, N. Mikami, Complete infrared spectroscopic characterization of phenol–borane-trimethylamine dihydrogen-bonded complex in the gas phase, J. Chem. Phys. 124 (2006) 241103.

[45] A. Fujii, T. Ebata, N. Mikami, An infrared study of π-hydrogen bonds in micro-solvated phenol: OH stretching vibrations of phenol–X ($\mathrm{X=C_6H_6}$, $\mathrm{C_2H_4}$, and $\mathrm{C_2H_2}$) clusters in the neutral and cationic ground states, J. Phys. Chem. A 106 (2002) 8554–8560.

[46] T. Sagara, E. Ganz, Calculations of dihydrogen binding to doped carbon nanostructures, J. Phys. Chem. C 112 (2008) 3515–3518.

[47] H. Ishikawa, A. Saito, M. Sugiyama, N. Mikami, First observation of a dihydrogen bond involving the Si–H group in phenol–diethylmethylsilane clusters by infrared-ultraviolet double-resonance spectroscopy, J. Chem. Phys. 123 (2005) 224309.

[48] C.P. Lau, S.M. Ng, G.-C. Jia, Z.-Y. Lin, Some ruthenium hydride, dihydrogen, and dihydrogen-bonded complexes in catalytic reactions, Coord. Chem. Rev. 251 (2007) 2223–2237.

[49] G.-J. Zhao, K.-L. Han, Novel infrared spectra for intermolecular dihydrogen bonding of the phenol–borane-trimethylamine complex in electronically excited state, J. Chem. Phys. 127 (2007) 024306.

[50] I. Alkorta, J. Elguero, S.J. Grabowski, How to determine whether intramolecular H···H Interactions can be classified as dihydrogen bonds, J. Phys. Chem. A 112 (2008) 2721–2727.

[51] M. Panda, K. Hofmann, M.H. Prosenc, B. Albert, Multi-centre, hydrogen and dihydrogen bonds in lithium *closo*-hydroborate obtained from liquid ammonia, Dalton Trans. (2008) 3956–3958.

[52] F. Furche, R. Ahlrichs, Adiabatic time-dependent density functional methods for excited state properties, J. Chem. Phys. 117 (2002) 7433–7447.

[53] J.L. Whitten, Coulombic potential energy integrals and approximations, J. Chem. Phys. 58 (1973) 4496–4501.

[54] B.I. Dunlap, J.W.D. Conolly, J.R. Sabin, On some approximations in applications of X_α theory, J. Chem. Phys. 71 (1979) 3396–3402.

[55] O. Vahtras, J.E. Almlöf, M.W. Feyereisen, Integral approximations for LCAO-SCF calculations, Chem. Phys. Lett. 213 (1993) 514–518.

[56] A. Schäfer, C. Huber, R. Ahlrichs, Fully optimized contracted Gaussian basis sets of triple zeta valence quality for atoms Li to Kr, J. Chem. Phys. 100 (1994) 5829–5835.

[57] R. Ahlrichs, M. Bär, H. Horn, C. Kölmel, Electronic structure calculations on workstation computers: the program system turbomole, Chem. Phys. Lett. 162 (1989) 165–169.

[58] V. Lemaur, M. Steel, D. Beljonne, J.-L. Brédas, J. Cornil, Photoinduced charge generation and recombination dynamics in model donor/acceptor pairs for organic solar cell applications: a full quantum-chemical treatment, J. Am. Chem. Soc. 127 (2005) 6077–6086.

[59] L.-C. Zhou, G.-J. Zhao, J.-F. Liu, K.-L. Han, Y.-K. Wu, X.-J. Peng, M.-T. Sun, The charge transfer mechanism and spectral properties of a near-infrared heptamethine cyanine dye in alcoholic and aprotic solvents, J. Photochem. Photobiol. A: Chem. 187 (2007) 305–310.

[60] L.-C. Zhou, J.-Y. Liu, G.-J. Zhao, Y. Shi, X.-J. Peng, K.-L. Han, The ultrafast dynamics of near-infrared heptamethine cyanine dye in alcoholic and aprotic solvents, Chem. Phys. 333 (2007) 179–185.

[61] S.-B. Wan, S.-S. Liu, G.-J. Zhao, M.-D. Chen, K.-L. Han, M.-T. Sun, Photoabsorption of green and red fluorescent protein chromophore anions in vacuo, Biophys. Chem. 129 (2007) 218–223.

[62] R.-K. Chen, G.-J. Zhao, X.-C. Yang, X. Jiang, J.-F. Liu, H.-N. Tian, Y. Gao, K.-L. Han, M.-T. Sun, L.-C. Sun, Photoinduced intramolecular charge transfer state in thiophene-π-conjugated donor–acceptor molecules, J. Mol. Struct. 876 (2008) 102–109.

[63] A. Usman, H. Masuhara, T. Asahi, Trans-cis photoisomerization of a photoactive yellow protein model chromophore in crystalline phase, J. Phys. Chem. B 110 (2006) 20085–20088.

[64] M. Suzuki, T. Asahi, H. Masuhara, Temperature dependence of ultrafast photoinduced ring-opening and -closure reactions of spironaphthooxazine in crystalline phase, J. Photochem. Photobiol. A: Chem. 178 (2006) 170–176.